

Variability of the Point Spread Function in the water column

Kenneth J. Voss

University of Miami, Physics Department
Coral Gables, Fl. 33124

ABSTRACT

The Point Spread Function (PSF) is an important property in predicting beam propagation and imaging system performance. An instrument to measure the *in situ* PSF of ocean water has been built and PSF profiles obtained. This instrument consists of two parts, a flashlamp with cosine emission characteristics, and an imaging solid state camera system. The camera system includes a thermoelectrically cooled CCD array with over 50 dB of dynamic range. This allows the camera to measure the steeply peaked PSF over short (10m) to long (80 m) ranges. Measurements of the PSF in three different locations are presented. One location was a coastal station off San Diego where the water column exhibited a well defined shallow (approximately 30 meter) mixed layer with a particulate maximum (defined by a maximum in beam attenuation) at the bottom of this layer. During these measurements the PSF was highly variable with depth, as was to be expected due to the dependence of the PSF on particle concentration and size distribution. In the second example the water column was almost homogeneous (as evidenced in the beam attenuation profiles). Hence, the PSF showed very little dependence on depth. Measurements of the variation of the PSF with range are also presented. A simple relationship of the variation of the PSF with angle and optical path length is presented.

1. INTRODUCTION

The seawater point spread function (PSF), is an important parameter in many problems of underwater imaging and transmission. It is an integral part of many models which predict image transmission^{1,2}. Its mathematical equivalent³, the beam spread function (BSF), is used in models of beam propagation.⁴ In theory, the very small angle scattering phase function can be derived from the PSF using the techniques of Wells⁵. This portion of the scattering phase function is very hard to measure by other methods. Measurement of the PSF, although important, has previously been reported for optical conditions of only limited variability⁶. Very few reported measurements of the small angle scattering phase function exist.⁷ Thus, the degree of variation of the PSF and also the small angle portion of the scattering phase function is virtually unknown. If one requires the PSF or BSF in modeling optical systems, direct measurement of the property is required.

The best definition of the PSF is given by Mertens and Replogle.⁶ In this paper they define the $PSF(\theta, \phi, R)$ as the apparent radiance of an unresolved Lambertian source at the position $(0,0,0)$

normalized to source intensity. This quantity has units of m^{-2} . In more physical terms, the PSF can be thought of as the image of a unresolved cosine source obtained with a camera and point source at opposite ends of the desired range. If there were no scattering, the PSF would be a delta function in the center of the camera image. Because of scattering, the image of the point source is blurred, and this blurring is equivalent to the PSF.

Wells⁵ showed theoretically that the PSF could be linked to the scattering function for the case of unpolarized light in the small angle limit. This derivation linked the PSF, modulation transfer function (MTF), and the scattering phase function. In this derivation the $PSF(\theta, \phi, R)$ was shown to be the 2 dimensional Fourier transform of the MTF. Or, since the PSF is rotationally symmetric ($PSF(\theta, \phi, R)$ is independent of ϕ), $PSF(\theta, R)$ is the Hankel transform of the MTF. In this formulation, the MTF is related to the scattering phase function by:

$$MTF(\psi, R) = \exp(-D(\psi)R)$$

where

$$D(\psi) = c - \Sigma(\psi),$$

$\Sigma(\psi)$ is the Hankel transform of the scattering phase function, c the beam attenuation coefficient, and ψ is the angular frequency. Physically $\Sigma(\psi)$ corresponds to a restoring function for the attenuation coefficient at low angular frequencies. $\Sigma(\psi)$ goes to 0 at high frequencies, while at low frequencies $\Sigma(\psi)$ goes to b_{forward} , the forward component of the scattering coefficient. This implies that $e^{-K_E d R} \approx MTF(\psi, R) \approx e^{-cR}$, where K_{Ed} is the downwelling irradiance diffuse attenuation coefficient. Therefore, with these theories, one can calculate the PSF given the volume scattering function (including the very small angle component) or given the PSF, one can calculate the small angle volume scattering function.

2. INSTRUMENTATION

The angular region that is of most interest in the PSF (or BSF) is on the order of 1 mrad, while minimum interesting ranges are usually on the order of 10 m. If measurements are to be performed by collecting individual data points, precise alignment between the source and detector must be maintained. When the measurements are required *in situ* and in many different water types this alignment is difficult or impossible to maintain. We have chosen a measurement method (first developed by Honey³) which avoids these problems. The technique involves use of a point source (a flashlamp) and a camera directed toward this point source. By using a camera, the measurements are reduced to a single image for the PSF distribution, and the problem of alignment is reduced to understanding the transformations relating object space to the image plane. However,

a camera system with sufficient dynamic range and resolution to measure the PSF over the angular and spatial range of interest is required.

The instrumentation and calibration procedures for our camera system are described in detail elsewhere⁸ however, a brief description of the system would be useful. The camera system on which our system is based includes a CCD camera and controller made by Photometrics, Ltd. The CCD array (Thompson CSF) in the camera system is thermoelectrically cooled to obtain very low noise rates (on the order of 10 thermally generated electrons per pixel). The array also has very deep electron wells (can contain 6×10^5 electrons per pixel) allowing a large dynamic range. The CCD is read using a 14 bit A to D converter, which takes advantage of the intrinsic dynamic range of the camera. A standard 35 mm camera lens was used (focal length 28mm), and the whole camera system was placed in a waterproof housing. A flat plate window was used and the air-glass-water interface refractive effects were taken into account in the calibration procedure. The flashlamp is a standard EG&G bulb type flashlamp, placed in an underwater housing. A cosine emitter was designed, following closely the design of cosine collectors,⁹ which produced the desired emission characteristics. The systems spectral response was limited by an interference filter placed in front of the camera lens. For the data presented in this paper, the filter was centered at 500nm and had a band pass of 10nm.

The system is used in two modes; fixed separation (or range) between the camera and flashlamp, and varied separation. The first mode is useful for obtaining profiles of the PSF through the water column. This is arranged by locking the flashlamp at a given distance below the camera on the hydrowire and then fixing the camera to the wire. This allows the separation to be maintained almost exactly. The second mode allows the variation of the PSF with range to be determined. This is arranged by locking the flashlamp to the hydrowire and allowing the camera to slide freely (with a separate support member) on the hydrowire. Keeping both units on the same wire helps to ensure that the flashlamp will be in the field of view of the camera even at larger wire angles. The shadowing caused by the wire can be neglected since it obstructs an insignificant portion of the solid angle of the image.

3. DATA

An example PSF measurement is shown in Figure 1. The central region, from 0 to 4 mrad in this case, is the image of the source. The values in this region should allow a measure of the beam attenuation. The region between 4 and 80 mrad, in this example, is the region for which the PSF measurement is correct. The region above 80 mrad is the noise floor in the camera system (values of the PSF in this region are significantly less than 1 camera count).

Data presented in this report were obtained from three locations, the Sargasso Sea (SS), Tongue of the Ocean (TOTO) Bahamas, and coastal Pacific Ocean (PO). The hydrodynamic structure of the SS and TOTO stations were very different from the PO station and this difference was observable in the optical properties of the water column. Sample beam attenuation profiles are

illustrated for the three locations in Figure 2. The most important feature is the relative homogeneity of the SS and TOTO stations compared to the PO station. The maximum in beam attenuation at approximately 30 meters was reflected in the profiles of the PSF.

Figure 3 illustrates the PO PSF at fixed separation (11m) and camera depths of 30, 40, and 50m. The PSF measurement integrates the optical properties of the region between the camera and flashlamp, i. e. the region between the camera and 11m below the camera in this case. As shown in Fig. 3, the slope of the PSF increases as the water between the camera and flashlamp becomes clearer. A good measure of the integrated optical properties between the camera and flashlamp is the total path optical length, τ , defined by:

$$\tau = \int_{z_1}^{z_2} c \, dz$$

where z_1 is the camera depth, z_2 the flashlamp depth, c the beam attenuation and dz the incremental depth. If the wire between the camera and flashlamp is at an angle θ with the vertical, then c must be multiplied by $\cos(\theta)$. For the measurements in Figure 3, the optical pathlengths were 4.6, 3.1, and 2.4 for the 30, 40, and 50m depths respectively.

The independence of the PSF on depth given a homogeneous water mass is illustrated by Figure 4. This figure is the SS PSF for fixed separation (14.6m) and camera depths of 12, 22, and 33m. As can be seen the PSF's are almost indistinguishable, falling right on top of each other. The optical pathlength for this case was 1.1 for all three measurements.

Another feature of the PSF is that it appears to be almost linear on the $\log(\text{PSF})-\log(\theta)$ graph in the region between 4 and 100mrad. This linearity implies a functional relationship of :

$$\text{PSF}(\theta) = K \theta^{-m}$$

where K is a constant, and $-m$ is the slope of $\log(\text{PSF})$ versus $\log(\theta)$. This provides a simple way of quantifying the change in the PSF with range or depth. This slope was calculated for measurements obtained at stations in the SS, PO and TOTO (the error in the slopes calculated was approximately 0.3 for the 95% confidence limit). For each of these measurements, τ was calculated using measurements of the beam attenuation profile (SS and TOTO measurements were provided by Jeff Smart¹⁰). Finally the slopes obtained were plotted versus τ and are shown in Figure 5. There are several features to note on this graph. First, the stations in all locations seem to follow the same relationship, thus implying that a general relationship can be developed which describes the variation of the PSF with τ . The second feature to note is that the relationship holds for optical pathlength, not range. This is illustrated by the PO data which was separated in the graph by range. Because of the inhomogeneity of the water column, the optical path lengths for different ranges were interspersed, and the slope, m , illustrates this dependence on τ .

At large distances, the radiance field from the point source in a scattering medium will become totally diffuse. At this point the PSF measured will be independent of angle, thus the slope calculated above will approach 0. Using this boundary condition a functional relationship of slope versus optical pathlength of the form $K \cdot 10^{-\beta \tau}$ was assumed. The data in Figure 5 was fit to a

relationship of this form illustrated in the graph as the solid line. The values determined for K and β were 2.07 and 0.0655 respectively (r^2 was determined to be 0.926 for this relationship).

4. CONCLUSIONS

The dependence of the PSF on optical path length is illustrated for several measurements in the Sargasso Sea, Tongue of the Ocean, and coastal Pacific Ocean. If a simple linear form for the variation of $\log(\text{PSF})$ with $\log(\text{angle})$ is assumed, the constants defining this variation can be shown to be dependent on optical path length. While these relationships do not show the differences in curvature between locations which the measurements illustrate, they permit simple approximations of the PSF for specific optical pathlengths to be determined. Further work is being performed to analyze the curvature differences in hopes of relating this to variations in the small angle scattering function. More work is also being done to test the approximate relationships at greater optical path lengths, in the case of larger ranges and water with larger beam attenuation coefficients.

5. ACKNOWLEDGEMENTS

This work was started while I was at the Scripps Institution of Oceanography, University of California. The instrumentation was developed with the support of the Ocean Optics program of ONR (ONR N00014-85-K-0005 and N00014-90-J-1505). Data collection was supported by this ONR contract and the Applied Physics Laboratory, Johns Hopkins University (APL, JHU). The beam attenuation profiles in the Sargasso Sea and Tongue of the Ocean stations were provided by APL, JHU. Albert Chapin was instrumental in the development and data collection stages of this project, and I would like to thank Roswell Austin for his help and guidance in this work.

6. REFERENCES

- 1) McGlamery, B. L. "Computer analysis and simulation of underwater camera system performance", Scripps Institution Of Oceanography, Ref. 75-2, 1975.
- 2) Jaffe, J. S. "A model-based comparison of underwater imaging systems", Ocean Optics IX, Marvin Blizzard Ed., Vol. 925, pp. 344-350, SPIE, Bellingham, 1988.
- 3) Honey, R. C. "Beam spread and point spread functions and their measurement in the ocean", Ocean Optics VI, S.Q.Duntley Ed., Vol.208, pp.242-248, SPIE, Bellingham, 1979.
- 4) Duntley, S. Q. "Underwater lighting by submerged lasers and incandescent sources", Scripps Institution of Oceanography, Ref. 71-1, 1971.
- 5) Wells, W. H. "Theory of small angle scattering" .AGARD, No. 61, NATO, 1973, pp. 3.3-1 - 3.3-19.

- 6) Mertens, L. A. and F. S. Replogle, Jr. "Use of point spread functions for analysis of imaging systems in water", *J. Opt. Soc. Am.*, v.67, no.8, pp.1105-1117, 1977.
- 7) Petzold, T. J. "Volume scattering functions for selected ocean waters", *Scripps Institution of Oceanography, Ref. 72-78*, 1972.
- 8) Voss, K. J. and A. Chapin "Measurement of the Point Spread Function in the Ocean", *Appl. Optics.*, 1990, in press.
- 9) Tyler, J. E. and R. C. Smith, *Measurements of spectral irradiance underwater*, (Gordon and Breach, New York, 1970).
- 10) Jeff Smart, Applied Physics Laboratory, Johns Hopkins University, unpublished data.

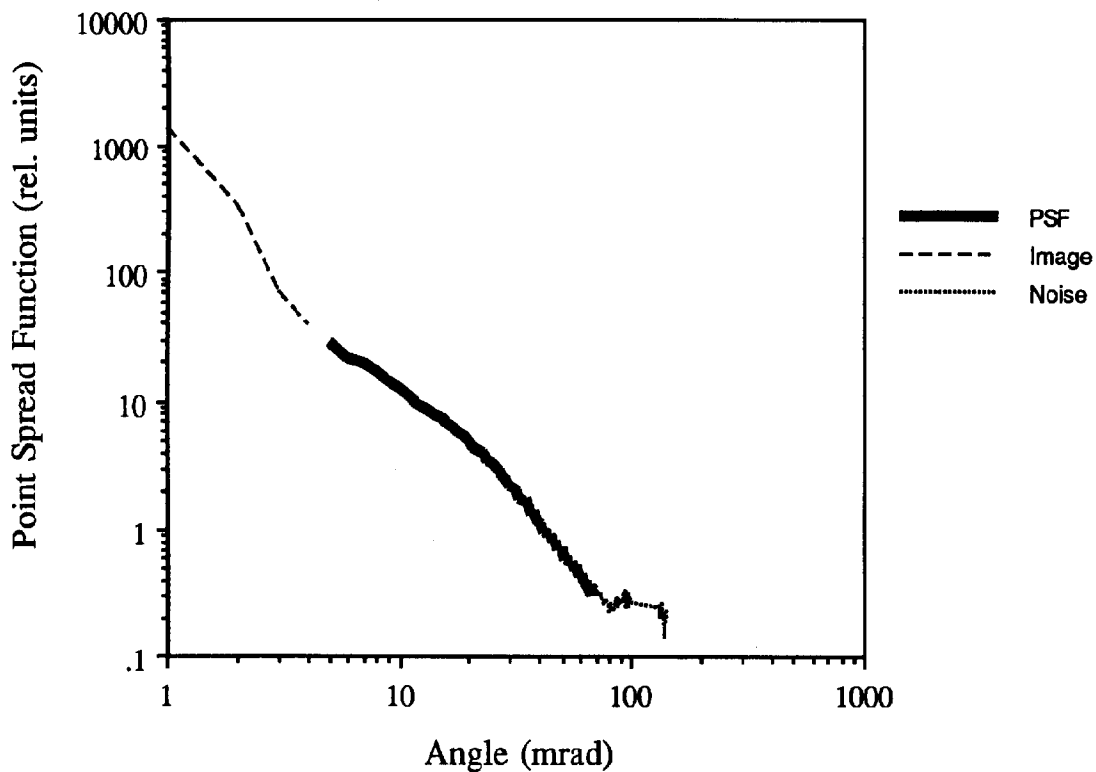


Fig. 1) Example PSF versus angle. Illustrates the different regions of the PSF measurement: the region from 0 to 4 mrad images the source, the PSF between 4 and 80mrad (in this example), and the region which is noise limited.

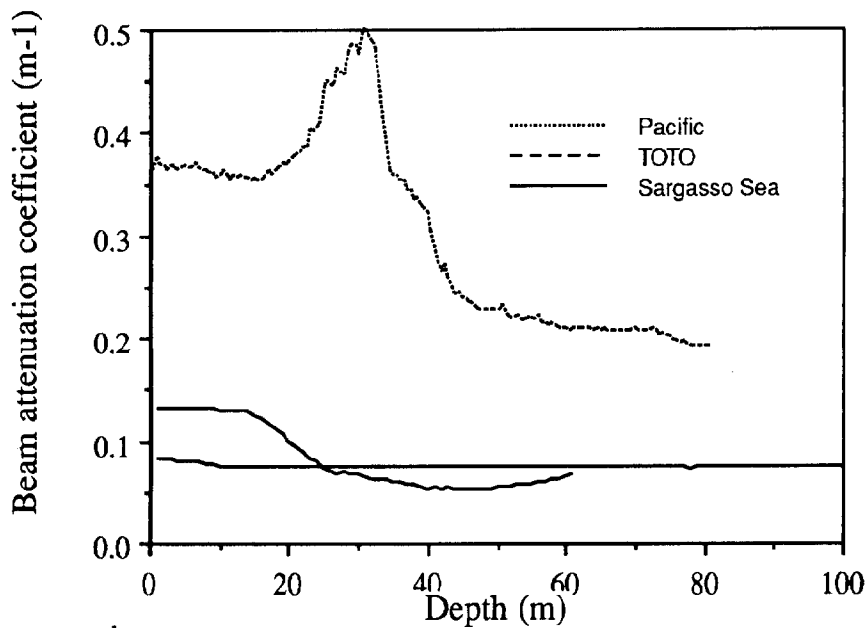


Fig. 2) Beam attenuation coefficient profiles at approximately 500nm. These profiles illustrate the differences in water column structure at these station locations.

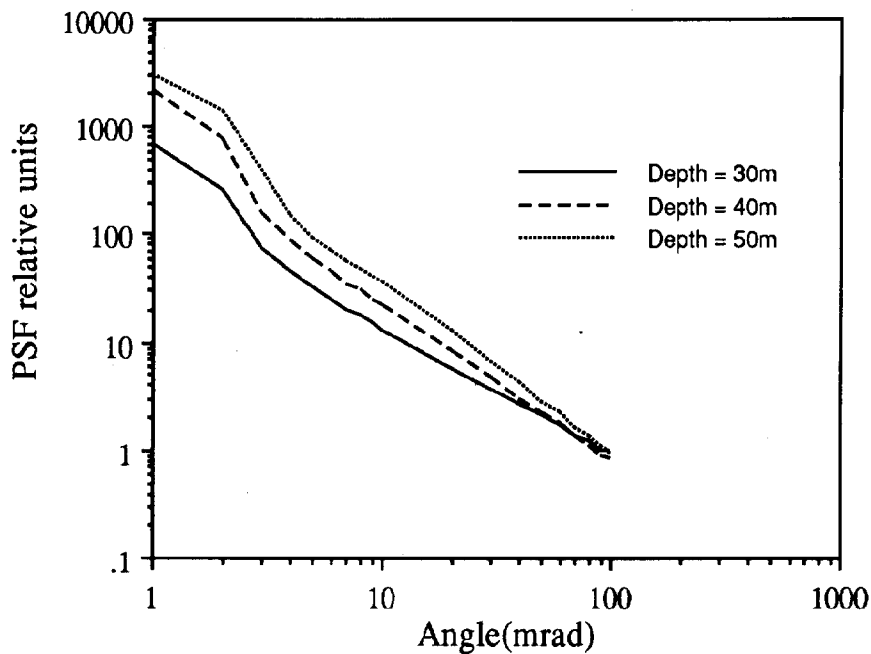


Fig. 3) PSF versus angle. Illustrates the variability of the PSF with depth, given an inhomogenous water column.

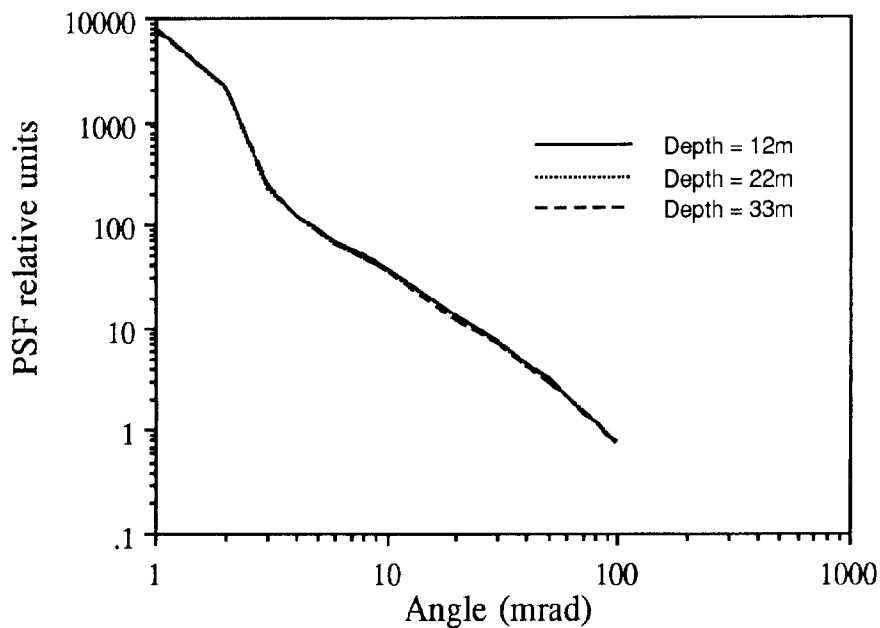


Fig. 4) PSF versus angle for Sargasso Sea station. As can be seen, due to the homogeneity of the water column, the PSF is constant with depth.

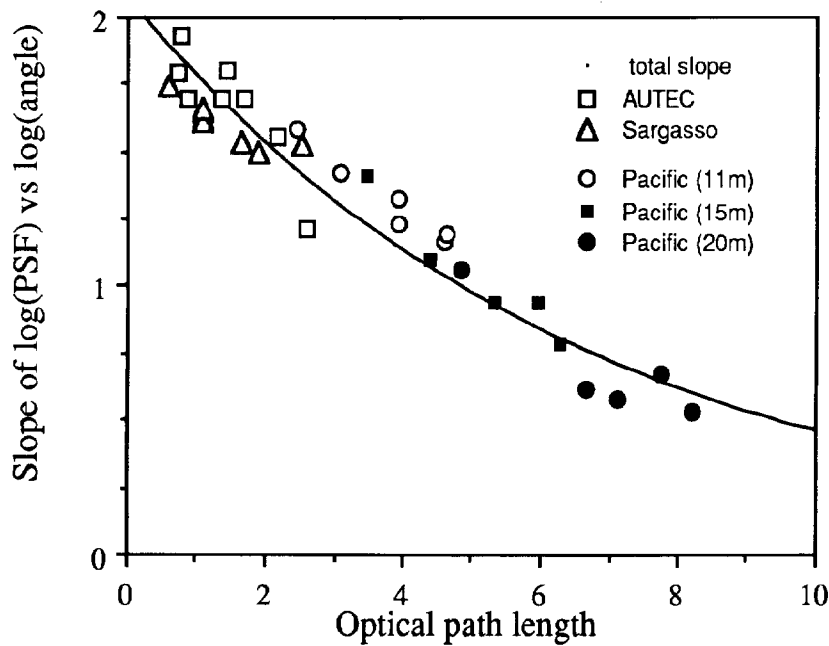


Fig. 5) Plot of Slope versus optical path length. Slope is determined from the individual PSF versus angle relationships, optical path is determined from the beam attenuation profiles. The line is a logarithmic fit to the data.